PUNCHING SHEAR STRENGTH AND DEFORMATION CAPACITY OF R.C. SLABS WITH DIFFERENT PATCH LOAD AREAS

Lect. Aamer Najim Abbas
Lecturer
amir_najim@yahoo.com

Dr. Husain Khalaf Jarallah
Lecturer
khalfdce@hotmail.com

Department of Civil Engineering
College of Engineering
Al-Mustansiriya University
Baghdad-Iraq

ABSTRACT

The main objective of this paper was to evaluate the effect of using different supporting areas or patch loads on a reinforced concrete slab within the slab-column connections. The increasing of the punching shear strength and deformation capacity when subjected to patch load was studied here. An experimental study was carried out on reinforced concrete slabs under a central patch load with circular, square and rectangular shapes of patch areas. A single concrete mix design was used throughout the test program. All of slab specimens were reinforced with distributed mesh reinforcement with equal steel ratios in both directions. The validation of the experimental work was made by analyzing the tested slabs by finite element method under cracking load. The results obtained by the finite element method were found to compare well with those obtained experimentally. In order to calculate the ductility for the tested slabs, the punching load has been determined by applying the published failure criterion and a load-rotation relationship obtained from semi-empirical relationship for the tested slabs. Conclusions on the influence of patch area on the punching shear capacity of reinforced concrete slabs were drawn. The experimental results confirm that the strength and deformation capacity are slightly influenced by the shape of the patch area. Among all specimens, the slabs with circular shape of patch area exhibited the best performance in terms of ductility and splitting failure.

KEYWORDS: concrete slabs; punching shear; patch load, ductility, finite element method.

مقاومة القص الثاقب وقابلية الهطول للبلاطات الخرسانية المسلحة تحت تاثير حمل البقعة وبمساحات تسليط مختلفة

م.عامر نجم عباس   م.د.حسين خلف جارالله
الجامعة المستنصرية /كلية الهندسة/قسم الهندسة المدنية

الخلاصة:

الهدف الرئيسي من هذا البحث هو تقييم تاثير شكل منطقة الاسناد على الاعمدة في البلاطات الخرسانية المسلحة ولمعرفة مقدار الزيادة في قوة القص ومقاومة التشوه في منطقة اتصال البلاطة الخرسانية مع العمود عند تسليط الاحمال. وقد أجريت دراسة

تجريبية على بلاطات خرسانية مسلحة تحت تحميل احمال بقعية مع شكل مختلف من منطقة التسليط. وقد تم استخدام نسب حديد متساوية بكلا الاتجاهين مع خرسانة تملك نفس المواصفات لجميع النماذج مع سمك متساوي. دقة النتائج المستحصلة من الدراسة العملية جاءت معقولة ومقبولة مقارنة بالنتائج التحليلية المستحصلة من التحليل باستخدام العناصر المحددة تحت الاحمال االتي تحدث عندها اول تشقق في خرسانة النماذج في منطقة الشد. تم تحديد الحمل الذي يتم حساب اليونة عند تسليطه باستخدام معادلة تم الحصول عليها من دراسات اخرى. النتائج العملية تؤكد ان شكل منطقة تاثير الاحمال يؤثر قليلا في مقاومة القص. كان الشكل الدائري لمنطقة التسليط اعطى أفضل أداء من حيث اليونة وفشل الخرسانة.

1. INTRODUCTION

In flat-plate floors, slab-column connections are subjected to high shear stresses produced by the transfer of the internal forces between the columns and the slabs (**ACI-421.1R-08, 2008; ACI-421.1-99, 1999**). Normally it is desired to increase the slab thickness or using drop panels or column capitals of exceptionally high strength for shear in reinforced concrete slab around the supporting column. Occasionally, methods to increase punching shear resistance without modifying the slab thickness are often preferred (**Cheng and Montesinos**, **2010**). The ways to transfer the force from column to the slab need to be studied to increase the shear resistance. Several reinforcement alternatives for increasing punching shear resistance of slab-column connections, including bent-up bars (**Hawkins et al., 1974; Islam and Park, 1976**), closed stirrups (**Islam and Park, 1976**), shearheads (**Corley and Hawkins, 1968**), and shear studs (**Dilger and Ghali, 1981**), have been evaluated in the past five decades. But there is a little experimental and theoretical information about the influence of patch area or cross section area shape for supporting column in the reinforced concrete shear resistance.

The main purpose of this paper is to introduce an experimental study about punching shear strength and deflection behavior of the reinforced concrete slab with different patch load areas. Validity of experimental cracking deflection results was checked by analyzing the tested slabs under cracking load using the finite element method. Accuracy of results of cracking deflections is found to be reasonable and acceptable. The load –rotation curve was obtained for the tested slabs by using published semi-empirical relationship (**Muttoni, 2003**).

2. EXPERIMENTAL PROCEDURE
The experimental result is discussed in this paper.

2.1 Materials
A total of three reinforced concrete slab specimens with loading areas of different shapes have been used in this study. A single concrete mix was used throughout the test program. The concrete which is used in the specimens consists of ordinary Portland cement, natural sand and crushed stone aggregate with maximum size of 10 mm. The water/cement ratio for concrete was 0.25. The mix proportions for cement, aggregate and water are given in **Table (1)**.

Deformed steel bars of diameter 5 mm were used in the slab panels. The bars are tested to determine the yield stress, ultimate stress and elongation. The test was carried out according to (**ASTM A615 / A615M, 2003**). The steel deformed bars having average yield strength and ultimate strength of 435MPa and 601MPa respectively.

2.2 Specimen Details
Details of the slab specimens are given in **Table (2)**. Details of slabs with reinforcement placements and patch load areas shown in the **Fig. 1**.

2.3 Compressive Strength

The code of practice assumes the punching shear resistance is proportional to the nth root of concrete strength **(ACI 318M-08, 2008; BS 8110-Part 1, 1997; NZS 3101-Part 1&2, 1982)**. In present work, standard cubes (150 mm) were used according to **(BS 1881: Part 116, 1983)** and they are de-molded one day after casting. Testing is carried out at (28) days age. The machine which is used in the tests is a hydraulic type of (3000) kN capacity. The average compressive strength of three cube samples was 41 MPa at 28 days.

3. TESTING PROCEDURE

3.1 Test Setup

The slabs are tested under one point load at mid-span as shown in **Fig. (2)**.The four sides of slabs were supported on bearing rollers on identical spreader plates. Four steel blocks were used at each corner of the slab as resting supports. These blocks to keep the clear span of 400 mm of all specimens. During testing, corner angles of each sample were properly anchored by means of heavy joist, which was connected to structural floor as shown in **Fig. (3)**. There was one dial gage at the mid-span to measure the central slab deflection as shown in **Fig. (4)**.

3.2 Test Procedure

Before testing, slabs were checked dimensionally, and detailed visual inspection made with all information carefully recorded. After setting and reading dial gage, loading was applied to specimen at an approximately constant rate, up to the peak load, at the same time deflections were measured. Deflection was measured at the center of tested slabs by means of (0.01 mm) dial gage, and readings from this gage were recorded for each load increment. Failure occurred abruptly in all specimens and loading was stopped after failure.

4. FINITE ELEMENT MODELING

The theoretical analysis was performed by the finite element package program **(SAFE, 2010)** under cracking load only. In this analysis, the shell elements are used. The stresses developed in this element are shown in **Fig. (5)**.The effect of membrane stresses were included in the finite element analysis of the slabs due to large deflection before punching shear failure. The edges of the slab were vertically restrained along four sides in the finite element model, as in the experimental setup. Further, in the finite element model, the loading was applied within the patch load area of central portion of slab model at the top surface to simulate actual experimental loading. For the finite element analysis, the effective flexural rigidity EI taken equal to $0.5E_cI_g$, in which E_c = Young's modulus of concrete, and I_g is the second moment of inertia of the gross section. The multiplier 0.5 is in accordance with the multiplier for beam stiffness in **(ACI 318M-08, 2008)**. The finite element meshed model of a typical slab is shown in **Fig. (6)**. The comparisons between the experimental and theoretical results of central deflection at cracking stage are shown in **Table (3)**. The results obtained by the finite element method are found to compare well with those obtained experimentally.

5. DISCUSSION ON TEST RESULTS

5.1 Observed Damage

At the end of each test, all models were flipped over in order to mark cracks on the bottom (tension) side of the slab. **Fig. (7)** shows the crack patterns at the failure stage for all three

specimens. All the models underwent punching type of failure. It has also been observed that the splitting failure with punching shear failure is more likely in slab with rectangular and square column because of the crack pattern for the main flexural cracks developed directly above the longitudinal reinforcement of all slabs with rectangular and square columns and that led to bond splitting before the punching shear failure.

The initial cracking of all the tested slabs was first observed in the tension zone of the slab near the column stub. In case of square and rectangular columns the initial crack was observed under the corner of column. The initial cracks appear in slabs with square and rectangular column faster than in case of circular column because high stress concentration in corners of columns. At this stage of loading the tensile stress in concrete reached the modulus of rupture value and cracking started in the zone of maximum tensile stress. The cracking load, failure load and failure mechanism for all tested specimens are presented in **Table (4)** below. The slab with rectangular columns gives minimum values for the cracking load because of the splitting failure.

5.2 Load versus Deflection Relationship

The punching shear load- displacement curves for all slabs are shown in **Fig. (8)**, and the failure punching shear loads are listed in **Table (4)**. According to these results, when the cracks start developing, deflections in the slabs increase at a faster rate, and continues to increase without an appreciable increment in load. Finally the deflection increases without any additional load and the dial gage starts to move very rapidly. The maximum deflection of slab with circular column is less than the slab with rectangular and square column. The load-deflection curves showed a slight difference in the deformation behavior under loading for all slabs. When a reinforced concrete slab is subjected to a gradual increase in load, the deflection increases linearly with the load in an elastic manner. After the cracks start developing, deflection in the slab increases at a faster rate. After cracks have developed in the slab, the load-deflection curve is approximately linear up to the yielding of flexural reinforcement after which the deflection continues to increase without an appreciable increment in load.

6. MOMENT CURVATURE CURVE

Moment-curvature analyses were carried out using the usual assumption that strains vary linearly across the depth of the section. Longitudinal reinforcement was modeled based on the measured material properties including strain-hardening. Unconfined concrete (the cover) was modeled based on stress-strain relations obtained from cubic tests. Moment-curvature calculations were carried out using the software section designer for (**ETABS, 2010**).In the moment curvature curve, the measured yield strength of the reinforcing steel and the cylinder compressive strength of the concrete were used. The moment curvature relationships for tested slabs thicknesses is given in **Fig. (9)**.

7. YIELD-LINE ANALYSIS

The flexural strength for moment curvature curve derived at ultimate strain for concrete moment has been used to derive the peak load in the yield line analysis. The expected flexural failure mechanism for simply supported slab with a point load at the center is illustrated in **Fig. (10)**.The relationship between the moment Strength and applied central peak load estimations using yield-line analysis is given as follow;

$$m = 0.12P \tag{3}$$

4

where m is the nominal flexural strength moment for the slab and P is the applied load.

Table (5) shows the experimental peak load and flexural capacity calculated from a yield-line analysis for each specimen. The load, normalized by the slab flexural capacity from the yield-line analysis, versus deflection response for the test specimens is presented in **Fig. (11)**.The result from a yield-line analysis gives a lower bound estimation of the strength of the slab due to the absence of the membrane action.

8. INFLUENCE OF PATCH LOAD AREA ON DEFLECTION CAPACITY

The effect of the patch area shape in the deflection capacity of the test specimens was evaluated through the ratio Δ_R/Δ_{Rc}, where Δ_{Rc} refers to the deflection of the specimen S1C with circular patch load area at peak load. Δ_R, on the other hand, is the deflection at peak load for each test specimen. The calculated values of Δ_R, Δ_{Rc} and Δ_R/Δ_{Rc} are given in **Table (6)**. Among all specimens, Specimens S3R exhibited the best performance with an increase of 36% in deflection capacity compared to Specimens S1C.

9. ENERGY ABSORPTION

Energy absorption capacity of the test specimens was evaluated based on the area under the normalized punching shear stress versus deflection response **(Cheng, 2009)**, where the vertical axis was selected as the normalized shear stress, $\text{Punching Load}/(b_o d \sqrt{f'_c})$ and the horizontal axis represents the vertical deflection **(Fig. (12))**, where; b_o = perimeter of critical section for shear (mm), d = distance from extreme compression fiber to centroid of longitudinal tension reinforcement (mm) and f'_c specified compressive strength of concrete cylinder (MPa). **Table (7)** summarizes the energy values were calculated according to the area under the curves shown in **Fig. (12)** for each specimen. It can be noticed that the specimens with rectangular patch area had better energy absorption ability.

10. LOAD-ROTATION RELATIONSHIP

The ductility of slabs failing in punching shear can be obtained by considering a suitable load-rotation relationship for the slab. **(Muttoni, 2003)** proposed semi-empirical formal to derive the load-rotation relationship for the slab as below;

$$\psi = 0.33 \frac{L}{d} \frac{f_y}{E_s} \left(\frac{V_d}{8\,m_{Rd}}\right)^{3/2} \tag{2}$$

where L is the span of the slab, m_{Rd} is the flexural capacity of the slab in the column region reduced by the strength reduction factor, f'_c specified compressive strength of concrete cylinder ; fy is yield strength of bending reinforcement; V_d load during testing , d = distance from extreme compression fiber to centroid of longitudinal tension reinforcement and ψ is slab rotation.
Still further, the following failure criterion was proposed for punching shear failures in slabs without transverse reinforcement **(Muttoni, 2008)**:

$$\frac{V_R}{\left(b_o\,d\,\sqrt{f'_c}\right)} = \frac{3/4}{\left(1+15\,\frac{\psi\,d}{d_{go}+d_g}\right)} \tag{3}$$

where dg_0 is a reference diameter of the aggregate admitted as 16mm; dg is the maximum diameter of the aggregate used in the concrete slab, in mm. Finally the ductility of the reinforced concrete slab under punching shear can be obtained by using curvature ductility as follow;

$$\mu_\psi = \frac{\psi_m}{\psi_y} \tag{4}$$

where ψ_m is the curvature at the end of the post elastic range and ψ_y is curvature at the first yield. In the present study the value ψ_m represents the curvature value for the intersection point between the failure criterion from equation (2) and the load-rotation from equation (1), as define shown in **Fig.(13)**. The Load-rotation curves and failure criteria for tested slab have been shown in **Fig. (14)**.Accordingly, the ductility values calculated and show in **Table (8)** for tested slabs.

11. CONCLUSIONS

The results and conclusions are summarized in the following:
1. With reference to punching shear strength, the experimental results presented within this paper confirm the influence of the patch area shape on the strength and deformation capacity of slabs.
2. Validity of the experimental results were checked by analyzing the tested slabs by finite element method under cracking load. The central deflection results obtained by the finite element method are found to compare well with those obtained experimentally.
3. The published failure criterion simultaneously determines the punching load and the rotation capacity of the slab and its ductility.
4. Circular column is needed to be use in order to preclude splitting failure in the slabs.
5. The shape of patch load area had a significant influence on the ductility for reinforced concrete slab. Higher ductility has been observed for slab with circular shape of patch load area.
6. The behavior of punching shear reinforcing systems is slightly influenced by the shape of patch load area.
7. The yield analysis and experimental results shows that the flexural behavior is slightly influenced by the shape of patch load area for reinforced concrete slab.
8. The slab with rectangular shape of patch area had better energy absorption ability because of the larger plastic rotations sustained, since this slab has shorter the length of span in direction that moments are being applied. This specimen showed larger deformation capacity.

12. REFERENCES

1. American Concrete Institute, ACI 421.1R-08, 2008,**"Guide to Shear Reinforcement for Slabs",** reported by joint ACI-ASCE Committee 421.

2. American Concrete Institute, ACI 421.1R-99, 1999,**"Shear Reinforcement for Slabs",** reported by joint ACI-ASCE Committee 421.

3. American Concrete Institute, ACI Committee 318, 2008,**"Building Code Requirements for Structural Concrete (ACI 318M-08) and Commentary"**, Forming ton Hill, Michigan, 107 PP.

4. ASTM Standards: A615/A615M-03, 2003, **"Standard Specification for Deformed and Plain Billet-Steel Bars for Concrete Reinforcement"**, ASTM International, 100 Barr Harbor Drive, West Conshohocken, PA 19428-2959, USA.

5. British Standards Institution, 1983, **"Method for Determination of Compressive Strength of Concrete Cubes (BS 1881: Part 116: 1983)"**, British Standards Institution, London.

6. British Standards Institution, 1997, **"Code of Practice for Design and Construction (BS 8110: Part 1: 1997)"**, British Standards Institution, London.

7. Cheng, M. and Montesinos, G., 2010, **"Evaluation of Steel Fiber Reinforcement for Punching Shear Resistance in Slab-Column Connections—Part I: Monotonically Increased Load"**, ACI Structural Journal, V. 107, No. 1, January-February.

8. Cheng, M., 2009,**"Punching Shear Strength and Deformation Capacity of Fiber Reinforced Concrete Slab-Column Connections under Earthquake-Type Loading"**, Ph.D. thesis, Department of Civil Engineering, The University of Michigan, USA.

9. Corley, W. G., and Hawkins, N. M., 1968, **"Shear Head Reinforcement for Slabs"**, ACI Journal, Proceedings V. 65, No. 10, Oct., pp. 811-82.

10. Dilger, W. H., and Ghali, A., 1981, **"Shear Reinforcement for Concrete Slabs"**, Journal of the Structural Division, ASCE, V. 107, No. ST12, pp. 2403-2420.

11. ETABS Plus Version 9.7.1, 2010, **"Extended 3-D Analysis of Building Systems"**, Computer and Structures, Inc., Berkeley, CA, USA.

12. Hawkins, N. M.; Mitchell, D.; and Sheu, M. S., 1974, **"Cyclic Behavior of Six Reinforced Concrete Slab-Column Specimens Transferring Moment and Shear"**, Progress Report 1973-74 on NSF Project GI-38717, Department of Civil Engineering, University of Washington, Seattle, WA, Sept.

13. Islam, S., and Park, R., 1976, **"Tests of Slab-Column Connections with Shear and Unbalanced Flexure"**, Journal of the Structural Division, ASCE, V. 102, No. ST3, pp. 549-569.

14. Muttoni, A., 2003, **"Shear and Punching Strength of Slabs without Shear Reinforcement"**, Beton-und Stahlbetonbau, V. 98, No. 2, Berlin, Germany, pp. 74-84. (in German).

15. Muttoni, A.,2008, **"Punching Shear Strength Of Reinforced Concrete Slabs Without Transverse Reinforcement"**, ACI Structural Journal, Farmington Hills, Mich., Vol. 105, No. 4, pp.440-450.

16. SAFE Version 12.3.1, 2010, **"Slab Analysis by the Finite Element Method"**, Produced and Distributed by Computers & Structures, Inc. ,1995 University Avenue, Berkeley, California 94704, USA.

17. Standards Association of New Zealand, 1982, **"Code of Practice for Commentary on: The Design of Concrete Structures (NZS 3101:1982, Part 1 and 2)"**, Standard Council, New Zealand.

Table 1: Mix Proportions

Cement kg/m^3	Sand kg/m^3	Gravel kg/m^3	Water kg/m^3
570	680	1040	143

Table (2): Specimen Details

Specimen	Dimensions of Slab Specimen (Lengthxwidthxthickness)mm	Patch Load Shape	Patch Load Area Dimension (mm)	Bottom Reinforcement in Each Direction (No.-mm Ø)
S1C	450x450x30	Circular	22 dia.	4-Ø5
S2S	450x450x30	Square	25x25	4-Ø5
S3R	450x450x30	Rectangular	15x32.5	4-Ø5

Table (3): Comparison of Central Deflection at Cracking Stage

Specimens	Cracking Load(kN)	Experimental Δ_{cr}(mm)	Theoretical Δ_{cr} (mm)	ΔExp./ ΔTheo.
S1C	5	0.74	0.72	1.03
S2S	7	0.85	1.12	0.76
S3R	4	0.56	0.51	1.10

Table (4): The Cracking Load, Failure Load and Failure Mechanism

Specimen	Cracking Load(kN)	Failure Load(kN)	Failure Mechanism

S1C	8	17	Punching Shear
S2S	7	16.5	Punching Shear(Splitting)
S3R	4	16.5	Punching Shear(Splitting)

Table (5) Strength Estimations using Yield-Line Analysis

Specimen	Peak Load(kN)	Peak Load for Yield-Line Analysis(kN)	Test/Yield-Line
S1C	17	10.7	1.59
S2S	16.5	10.7	1.54
S3R	16.5	10.7	1.54

Table (6): Comparison of Deflection Capacities

Specimens	Δ_R (mm)	Δ_R/Δ_{Rc}
S1C	10	1.0
S2S	12.5	1.25
S3R	13.6	1.36

Table (7): Energy Absorption

Specimens	Normalized Energy	Energy/S1C Energy
S1C	6.27	1.0
S2S	6.44	1.03
S3R	6.74	1.07

Table (8): Ductility

Specimens	ψ_m %	ψ_y %	μ_ψ
S1C	1.215E-04	6.379E-06	19.05
S2S	1.162E-04	10.005E-06	11.61
S3R	1.162E-04	9.9234E-06	11.71

450 mm

400 mm

450 mm

400 mm

4-Ø5 each way

Loading block
(Patch area)

X

X

(a) Plane View

4-ϕ5 mm each
way

Loading block (Patch area)

Smooth Rod
(25 mm)

30 mm

(b) Section X-X
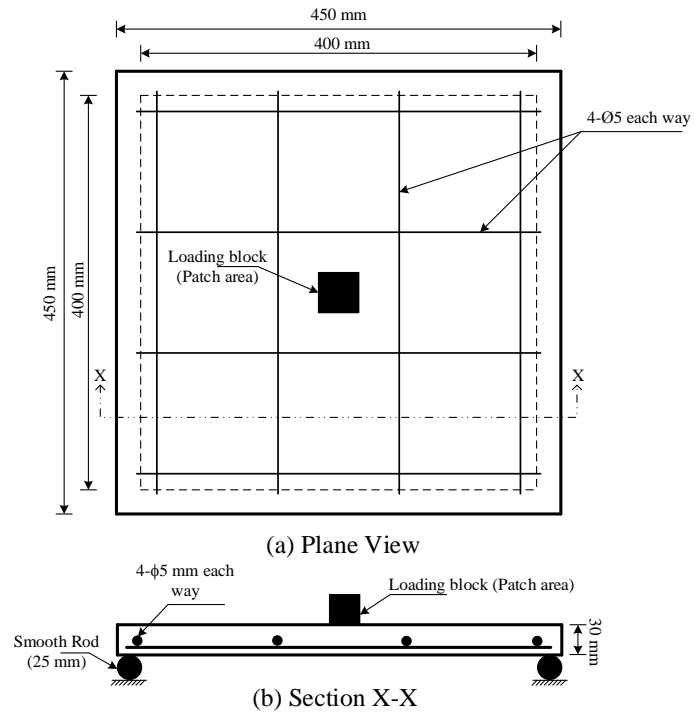
Fig. (1): Details of a Typical Model of Slab with Reinforcement.

Fig. (2): Test Setup.

Fig.(3): Support of the Test Setup.

Fig. (4): One Dial Gauges are Below the Center of Slabs.
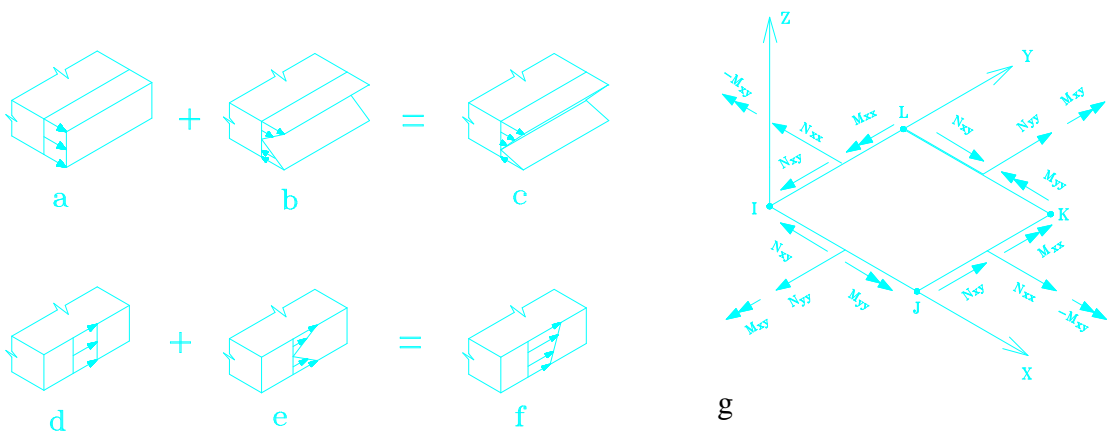
Fig.(5): Three Dimensional Plane Shell Element (a- Axial Stress, b- Bending Stress, c- Total In-plane Stress, d- Shear Stress, e- Twisting Stress, f- Total Shear Stress, g- Stress Conventions for Thin Plane Shell Element).
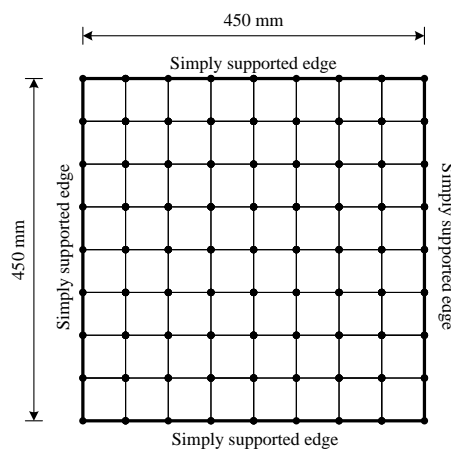
Fig. (6): Mesh Modelling of a Typical Slab.
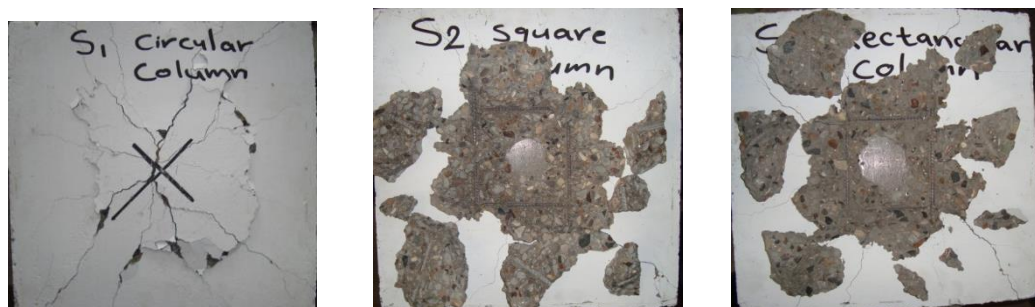
Fig. (7): Cracking Pattern on the Bottom Surface of a Model Slab.
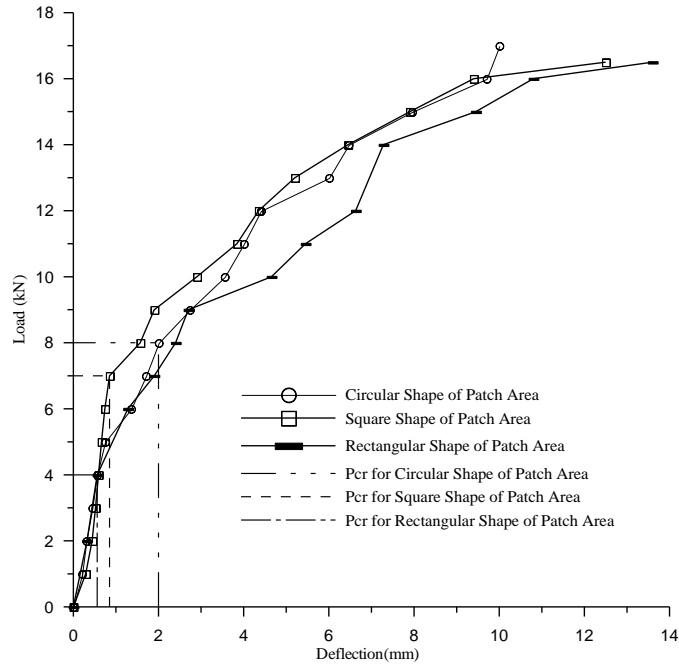
Fig. (8): Load-Deflection Curves of Tested Model.
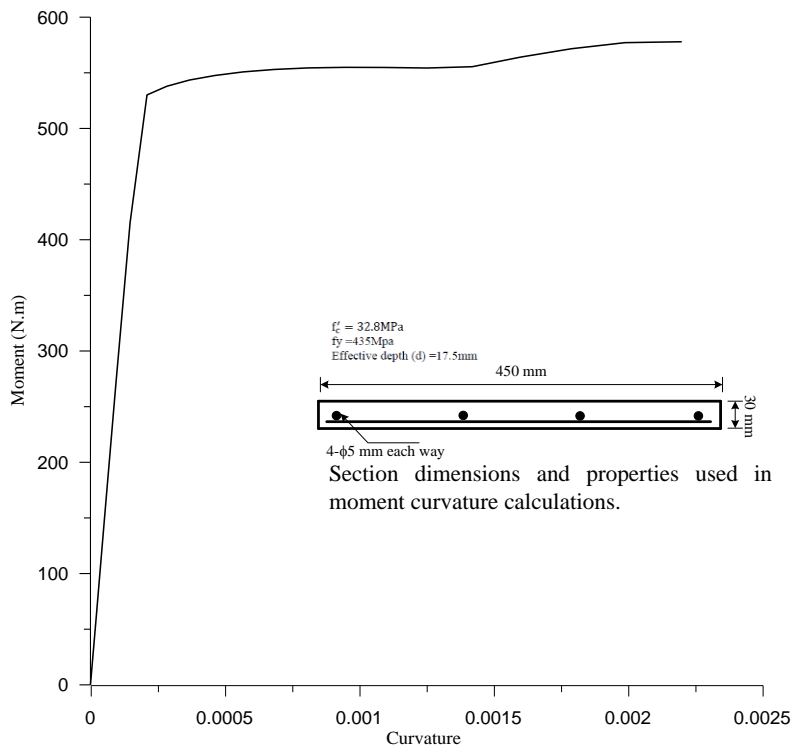
Fig. (9): Moment Curvature Curves.
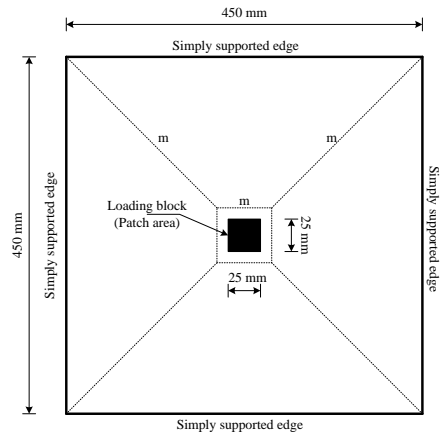
Fig. (10) Assumed Yield-Line Pattern for Test Specimens.
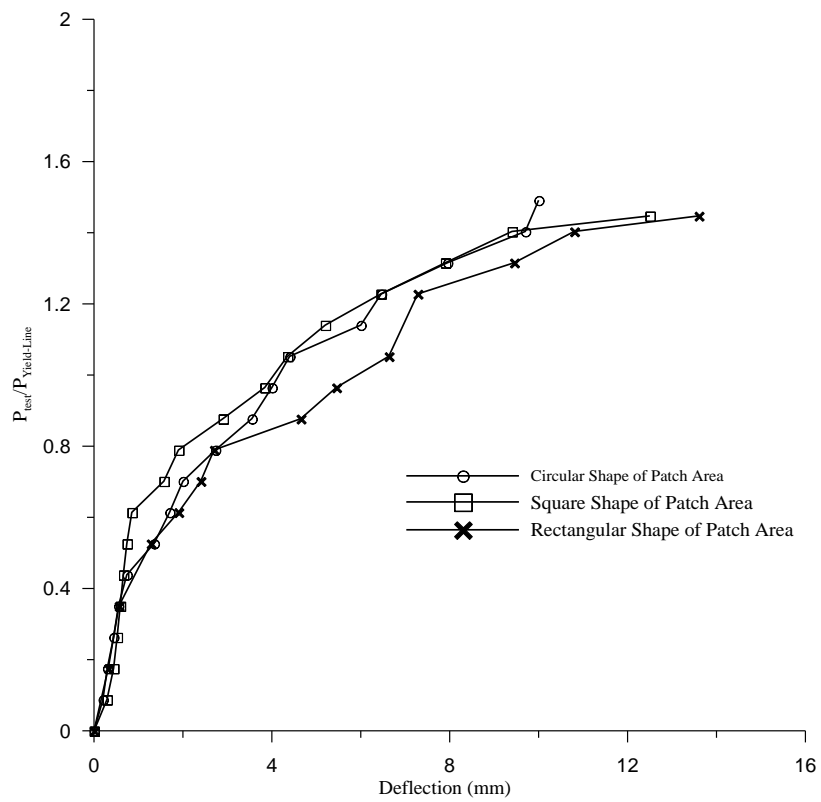
Fig. (11) Normalized Load versus Deflection Response.
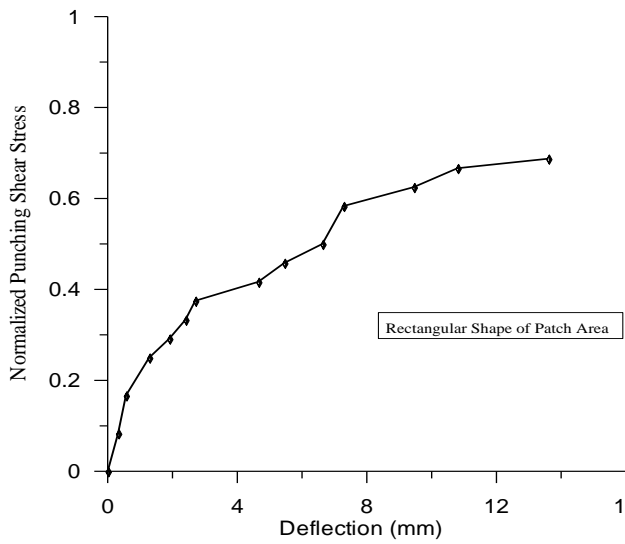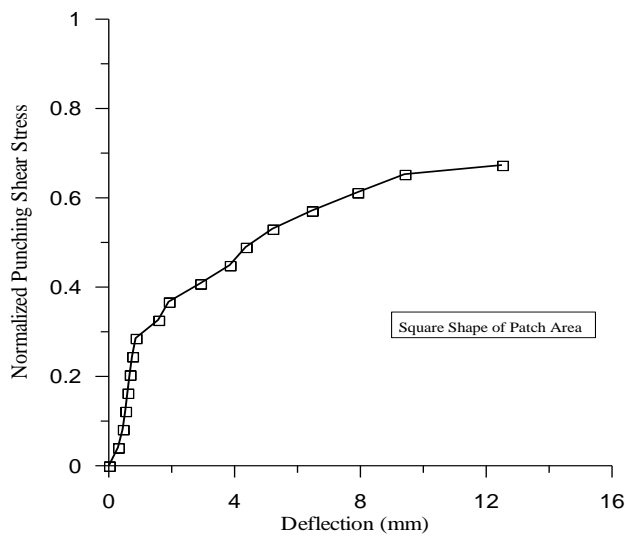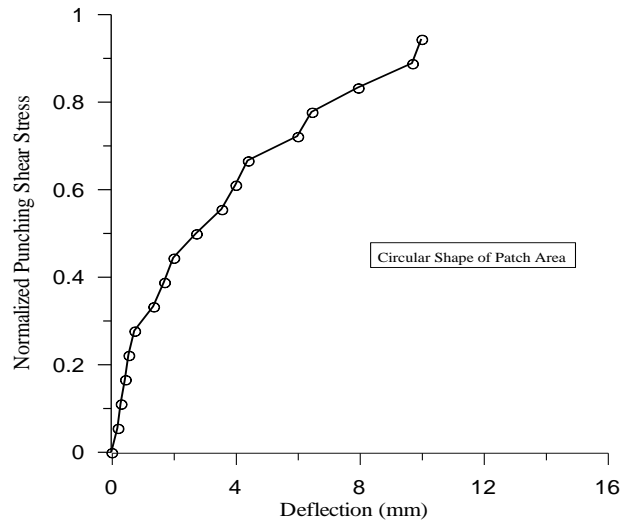
Fig. (12): Punching Load$/\left(b_o d \sqrt{f_c'}\right)$ and the Vertical Deflection Curve.
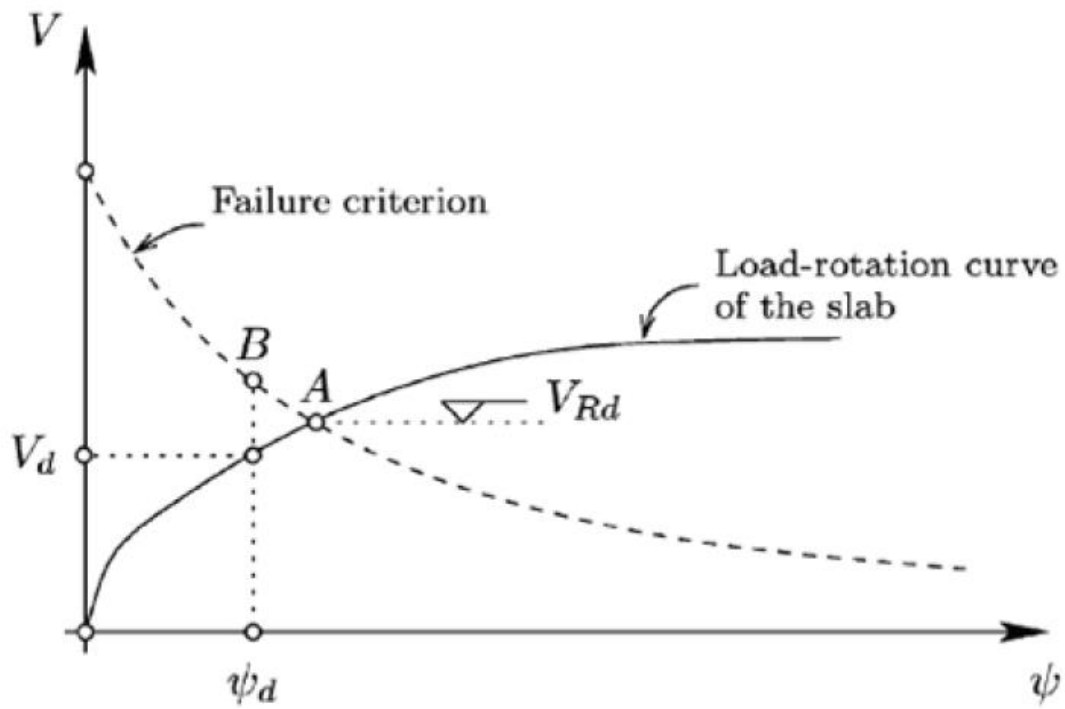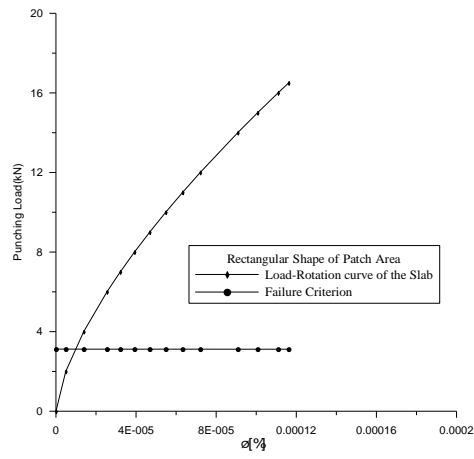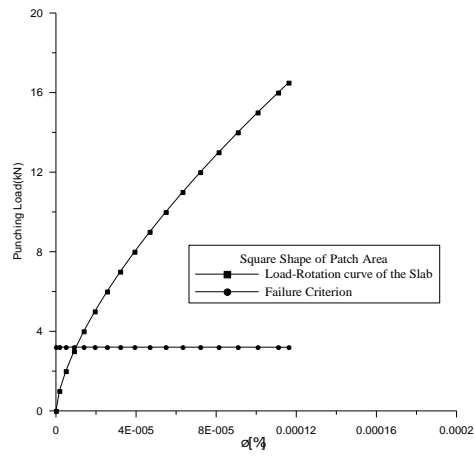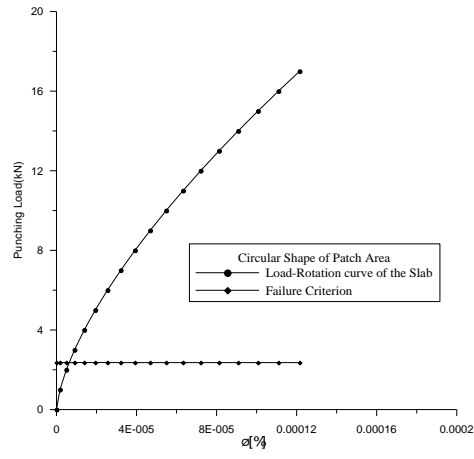
Fig. (13): Design Procedure to Check The Punching Strength of a Slab (Muttoni, 2008).

Fig. (14): Load-Rotation Curves and Failure Criteria for Tested Slabs.